

# Finite Element Analysis of Micro – Electro – Mechanical Systems: Towards the integration of MEMS in design and robust optimal control schemes of smart microstructures.

JOHN K. SAKELLARIS

Faculty of Applied Mathematics and Physics  
National Technical University of Athens  
9, Heroon Poytechniou, 15780 Zografou  
GREECE  
jsakel@central.ntua.gr

*Abstract:* - Microelectromechanical Systems (MEMS) is the technology of the very small, and merges at the nano-scale into "Nanoelectromechanical" Systems (NEMS) and Nanotechnology. MEMS are also referred to as micro machines, or *Micro Systems Technology (MST)*. MEMS are separate and distinct from the hypothetical vision of Molecular nanotechnology or Molecular Electronics. MEMS generally range in size from a micrometer (a millionth of a meter) to a millimeter (thousandth of a meter). At these size scales, the standard constructs of classical physics do not always hold true. Due to MEMS' large surface area to volume ratio, surface effects such as electrostatics and wetting dominate volume effects such as inertia or thermal mass. Finite element analysis is an important part of MEMS design. The paper presents the design of a vibration control mechanism for a beam with bonded piezoelectric sensors and actuators and an application of the arising smart structure for vibrations suppression too. The mechanical modelling of the structure and the subsequent finite element approximation are based on Hamilton's principle and classical engineering theory for bending of beams in connection with simplified modelling of piezoelectric sensors and actuators. Two control schemes LQR and  $H_2$  are considered. The latter robust controller takes into account uncertainties of the dynamical system and moreover incompleteness of the measured information, it therefore leads to applicable design of smart structures. The numerical simulation shows that sufficient vibration suppression can be achieved by means of the proposed general methods. It is given as a perspective to the MEMS technology towards the direction of integrating MEMS in design and robust optimal control schemes.

*Key-Words:* - Finite Element Analysis, Micro – Electro – Mechanical Systems, ANSYS software, Coupled problems, Micro - actuator, Bi - stable electromagnetic actuation, UV-LIGA technology, Simulation, Active structural control, Smart beam, Composite structure, Piezoelectric layer.

## 1. Introduction

Micro-electro-mechanical systems (i.e., MEMS) are integrated systems of microelectronics (IC), microactuator and, in most cases, microsensors [1]. MEMS technology offers unique advantages including miniaturization, mass fabrication and monolithic integration with microelectronics, and makes it possible to fabricate small devices and systems with high functionality, precision and performance. More important, MEMS technology can enable new circuit components and new functions [2] and [3]. Therefore, MEMS have attracted considerable attention since 1987 [1]. Microactuators are the key part of MEMS. For many MEMS devices such as switches, optical attenuators, pumps, valves, etc., microactuators are required to realize their physical functions. The controlled actuation or motion of microactuators can be achieved by several kinds of actuation mechanisms. Electrostatic, piezoelectric, magnetostrictive, magnetic, thermomechanical

actuators have been reported [4], [5], [6], [7] and [8]. Among the different actuation principles, the electrostatic actuation is predominantly employed for the electrostatic microactuators' characteristics of simple structures, small energy loss and being compatible with integrated circuit processes [9] and [10]. However, electrostatic actuation mechanism has the disadvantages of high driving voltage and small displacement [11]; the high driving voltage has an adverse effect on the lifetime of devices [12].

The electromagnetic actuators have received much attention for their capabilities of realizing both large force and displacement and suitability in harsh environment [13] and [14], thus electromagnetic actuators with various structures have been fabricated [7], [15] and [16]. Compared with electrostatic microactuators, the electromagnetic ones increase the displacement with low actuation voltage that can effectively enhance the stability of the devices. The disadvantage of such devices is that they have higher

power consumption, which is obviously an unfavorable factor for the heat dissipation of the microactuators with a compact structure. The high power consumption mainly comes from holding the state of the devices. To overcome the disadvantage above, electromagnetic actuation with bistable mechanisms was suggested. A type of latching electromagnetic microactuator with two stable states for reducing power consumption has been demonstrated by Ruan et al. [17]. The device was based on preferential magnetization of a permalloy cantilever in a permanent external magnetic field. But the force for the stable states came from the magnetizing cantilever in a magnetic field, which led to a low efficiency of electromagnetic effect. Ren and Gerhard [18] reported a bistable magnetic microactuator, where the device employed lateral movement and the motion was based on the bending of the cantilever. In this paper, an electrical - thermal MEMS microactuator will be presented.

## 2. Microsystem Analysis Features

ANSYS Multiphysics has an extremely broad physics capability directly applicable to many areas of microsystem design. Coupling between these physics enables accurate, real world simulation of devices such as electrostatic driven comb drives.

The ability to compute fluid structural damping effects is critical in determining the switching response time of devices such as micromirrors.

Electro-thermal-structural effects are employed in thermal actuators.

Fluid (CFD) capabilities are used to compute flow and free surface droplet formation useful in the design of ink-jet printer nozzles, and lab-on-chip applications.

The following figure (Fig. 1) explains how ANSYS Multiphysics capabilities fits into the Microsystem/MEMS design process:

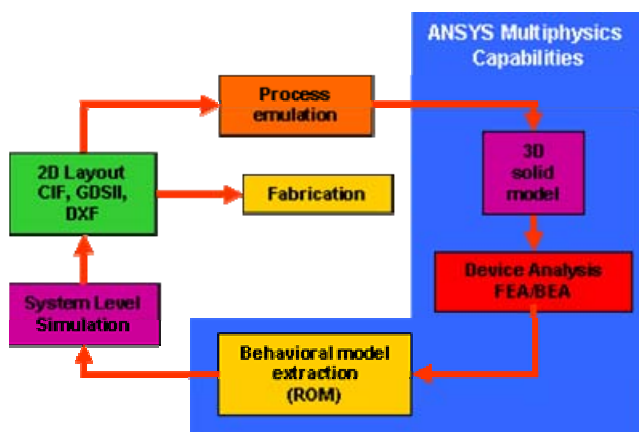


Fig. 1: ANSYS Multiphysics integration into the Microsystem/MEMS design process.

A sample of the features included in ANSYS Multiphysics are listed below:

- 1 Structural static, modal, harmonic, transient mechanical deformation.
- 2 Large deformation structural nonlinearities.
- 3 Full contact with friction and thermal contact.
- 4 Linear & non linear materials.
- 5 Buckling, creep.
- 6 Material properties: Temperature dependent, isotropic, orthotropic, anisotropic.
- 7 Loads/Boundary conditions: Tabular, polynomial and function of a function loads.
- 8 Plasticity, viscoplasticity, phase change.
- 9 Electrostatics & Magnetostatics.
- 10 Low Frequency Electromagnetics.
- 11 High Frequency Electromagnetics. (Full wave, frequency domain).
- 12 Circuit coupling - voltage & current driven.
- 13 Acoustic - Structural coupling.
- 14 Electrostatic-structural coupling.
- 15 Capacitance and electrostatic force extraction.
- 16 Fluid-Structural capability to evaluate damping effects on device response time.
- 17 Microfluidics: Newtonian & non Newtonian continuum flow
- 18 Free Surface VOF with temperature dependent surface tension.
- 19 Charged particle tracing in electrostatic and magnetostatic fields.
- 20 Electro-thermal-structural coupling.
- 21 Piezoelectric & Piezoresistive transducers: Direct coupled structural-electric physics. Full isotropic, orthotropic parameters.
- 22 Advanced thermoelectric effect such as Seebeck, Peltier & thermocouple.

## 3. ANSYS MEMS Applications Overview

ANSYS Multiphysics can be applied to a broad range of Microsystem/MEMS analysis. The following table (Tab. 1) shows the analysis capability relevant for a range of applications.

Microsystem Application	ANSYS Multiphysics Capability
Inertial Devices: Accelerometers & Gyroscopes	Structural modal, Static, Transient, Electrostatic-Structural, Reduced order macro modeling for system level.
Surface Acoustic Wave Devices	Acoustic - Structural coupling
MicroStripline Components	High Frequency electromagnetics.
Micro-patch and Fractal Antennas	High Frequency electromagnetics.
Piezo Inkjet Printheads	Thermal actuation: Electro-thermal - structural coupled physics. Thermal-structural coupled physics
Thermal Inkjet Printheads	Piezoelectric actuation: Direct coupled structural-electric physics. VOF Free surfaces & capillary action.
Micro mass spectrometers	Electromagnetics & charged particle tracing
Electrostatic comb drives	Electrostatic - structural coupling. Capacitance extraction.
Microfluidic Channels	Newtonian/non-Newtonian continuum flow
Piezoelectric actuators	Full isotropic & orthotropic parameters
Pressure transducers:	Capacitance based: Electrostatic structural coupling. Piezo-resistive based: Electro-Structural indirect coupling
Electromechanical RF filters	Electrostatic - structural coupling. Capacitance extraction.
Micromirror technology	Electrostatic - structural coupling. Fluidic structural capability to evaluate damping effects
Micro-grippers	Electro-Thermal-structural
Micro TIP field emitters	Electrostatics & charged particle tracing
Micro-Gear assemblies	Mechanical with complex contact, friction.
Thermoelectric actuators	Electro-thermal - structural coupled physics
Magnetostrictive actuators	Low Frequency electromagnetics

Tab. 1: The analysis capability of ANSYS relevant for a range of applications

## 4. Problem Definition

This paper demonstrates how to analyze an electrical-thermal actuator used in a micro-electromechanical system (MEMS). The thermal actuator is fabricated from polysilicon and is shown below.

The thermal actuator works on the basis of a differential thermal expansion between the thin arm and blade.

The required analysis is a coupled-field multiphysics analysis that accounts for the interaction (coupling) between thermal, electric, and structural fields.

A potential difference applied across the electrical connection pads induces a current to flow through the arm and blade.

The current flow and the resistivity of the polysilicon produce Joule heating ( $I^2R$ ) in the arm blade.

The Joule heating causes the arm and the blade to heat up.

Temperatures in the range of 700 - 1300°K are generated.

These temperatures produce thermal strain and thermally induced deflections.

The resistance in the thin arm is greater than the resistance in the blade.

Therefore, the thin arm heats up more than the blade, which causes the actuator to bend towards the blade.

The maximum deformation occurs at the actuator tip. The amount of tip deflection (or force applied if the tip is restrained) is a direct function of the applied potential difference.

Therefore, the amount of tip deflection (or applied force) can be accurately calibrated as a function of applied voltage.

These thermal actuators are used to move micro devices, such as ratchets and gear trains.

Arrays of thermal actuators can be connected together at their blade tips to multiply the effective force.

The main objective of the analysis is to compute the blade tip deflection for an applied potential difference across the electrical connection pads.

Additional objectives are to: Obtain temperature, voltage, and displacement plots, Determine total current and heat flow.

### 5.1 Given

Dimensions are in micrometers. The thermal actuator has an overall length of approximately 250 micrometers, and a thickness of 2 micrometers.

The given potential difference across the electrical connection pads is 5 volts. In Tab.2 are given the

characteristic magnitudes of the actuator

Material Properties for Polysilicon	
Young's modulus	169e3 GPa
Poisson's ratio	0.22
Resistivity	2.3e-5 ohm- $\mu$ m
Coefficient of thermal expansion	2.9e-6/ $^{\circ}$ K
Thermal conductivity	150e6 W/ $m^{\circ}$ K

Tab. 2: Characteristic magnitudes of the actuator

### 5.2 Approach and Assumptions

Coupled-field problems can be solved using the direct method or the sequential method. The direct method performs the coupled-field analysis in one step using coupled-field elements. The sequential method performs the coupled-field analysis in multiple steps, where the results from one step are used as input to the next step. Coupled field elements are not required for the sequential method. This paper uses the direct method to evaluate the actuator. The direct approach is the most efficient method for this problem. However, if it were necessary to include the effects of temperature-dependent material properties and/or thermal radiation, it would probably be more efficient to use the sequential method. The nonlinear thermal-electric problem could be solved using SOLID98 elements with only the TEMP and VOLT degrees of freedom active, and the mechanical problem could be solved using SOLID92 elements. The temperatures calculated in the thermal analysis could be applied as loading to the mechanical model using the LDREAD command.

It must defined the element type as SOLID98 using the default degrees of freedom [KEYOPT(1)]: UX, UY, UZ, TEMP, VOLT, MAG. The element simulates the coupled thermal-electric-structural response. The MAG degree of freedom is not required for this analysis so it will not be assigned a magnetic material property.

To define material properties for this analysis, it must be converted the given units for Young's modulus, resistivity, and thermal conductivity to  $\mu$ MKSV units. The units have been converted to  $\mu$ MKSV, and are shown in the following table (Tab. 3).

Material Properties for Polysilicon ( $\mu$ MKSV units)	
Young's modulus	169e3 MPa
Poisson's ratio	0.22
Resistivity	2.3e-11 ohm- $\mu$ m
Coefficient of thermal expansion	2.9e-6/ $^{\circ}$ K
Thermal conductivity	150e6 pW/ $\mu$ m $^{\circ}$ K

Tab. 3: Units' conversion

Next, the model is meshed with the coupled field elements. Then, voltages are applied to the electrical connection pads and set their temperature to an assumed 30 $^{\circ}$ C. Next, the electrical connection pads are mechanically fixed in the X, Y, and Z directions. Finally, the solution is obtained and post processing of the results to achieve the analysis objectives, as stated above.

## 6. Results

The geometry to be modelled appears in the next figure (Fig. 2):

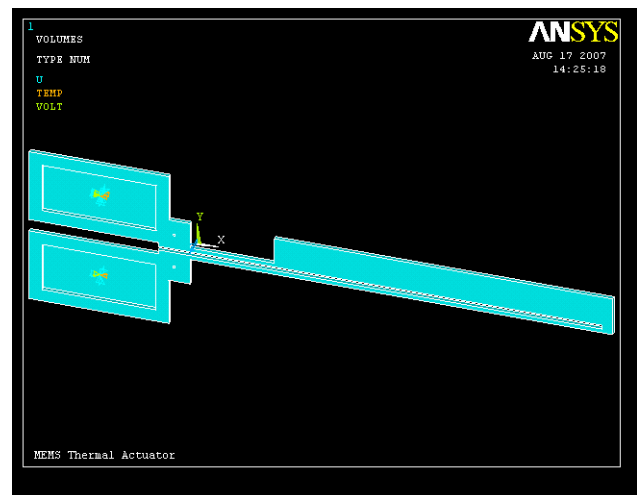


Fig. 2: Geometry to be modelled

The next figure presents a zoom of meshing (Fig. 3):

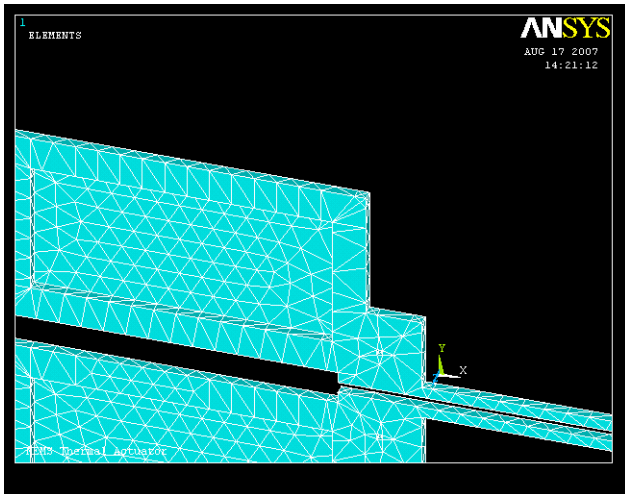


Fig. 3: Zoom of meshing

First, the temperature results will be plotted. This is one of the objectives of this analysis (Fig. 4):

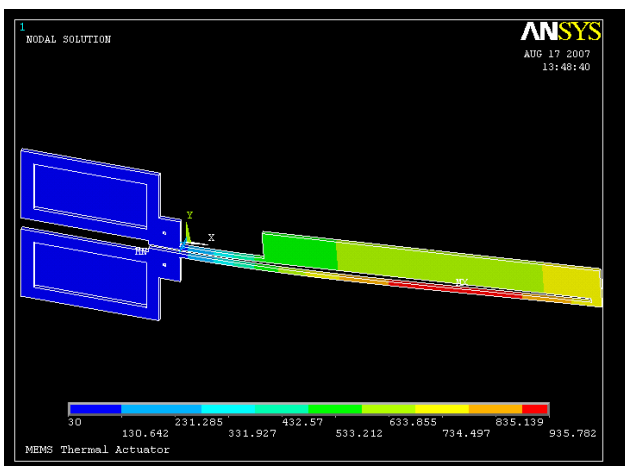


Fig. 4: Temperature results

It may be noted, that the electrical connection pads are the same color, reflecting the constant temperature boundary condition. It may be noted, also, that there is a change in color in the blade, as viewed from the pads end to the blade tip end, indicating that the voltage difference across the pads causes a temperature difference across the blade. Finally, it may be noted, that the thin arm is at higher temperatures than the blade.

Next, the voltage results will be plotted (Fig. 5):

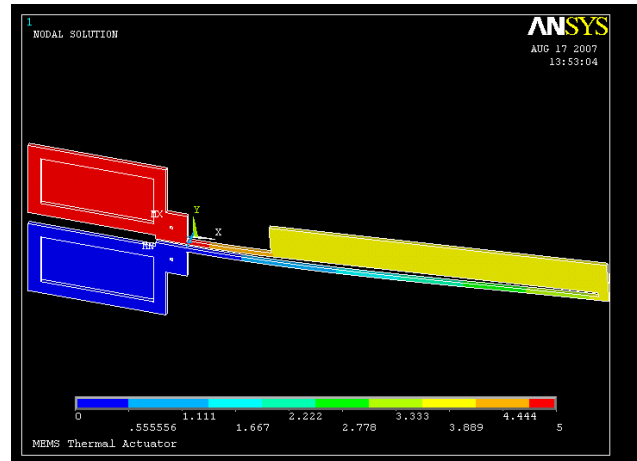


Fig. 5: Voltage results

It may be noted, that the electrical connection pads are distinctly two different colors, reflecting the voltage difference across the pads. It may be noted, also, that there is a change in color in the blade, as viewed from the pads end to the blade tip end, indicating that the voltage drop from pad 1 to pad 2 is distributed along the electrical conduction path of the actuator.

Finally, the displacement results will be plotted and more precisely those according to the Y – direction (Fig. 6):

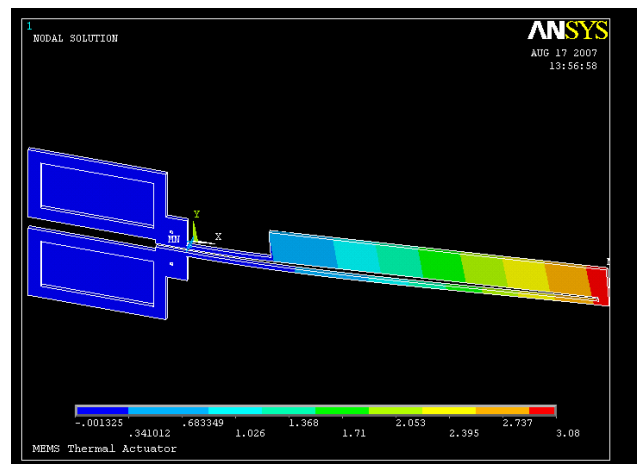


Fig. 6: Displacement results will be plotted and more precisely those according to the Y – direction.

It may be noted, that the electrical connection pads are the same color, reflecting that the pads are constrained in all directions. It may be noted, especially, the gradual change in color in the blade and thin arm, as viewed from the pads end to the blade tip end.

It may be noted, also, from the legend that the colour

of the tip of the blade indicates a deflection of approximately 3.07 micrometers. This deflection results from the 5 volts applied across the pads. The total heat flow is approximately  $8.07e9$  pW and the total current is approximately  $3.23e9$  pA.

### 7. An example of MEMS use: The deformable mirrors for adaptive optics [19]

The adaptive mirrors allow the correction of defects provoked by big telescopes. Their miniaturization will lead to a considerable gain as far as it concerns their weight and their dimensions, no matter how these instruments are used. Their resolution is increased, in this way. In the Laboratoire d'Electrotechnique de Grenoble a deformable mirror was developed based on an elastic membrane, on which micro – magnets are bonded and which are actuated by a network of planar windings. An example of using a deformable mirror will be given in (Fig. 7):



Fig. 7: An example of using a deformable mirror

The mechanical deformation of a deformable mirror will follow (Fig. 8):

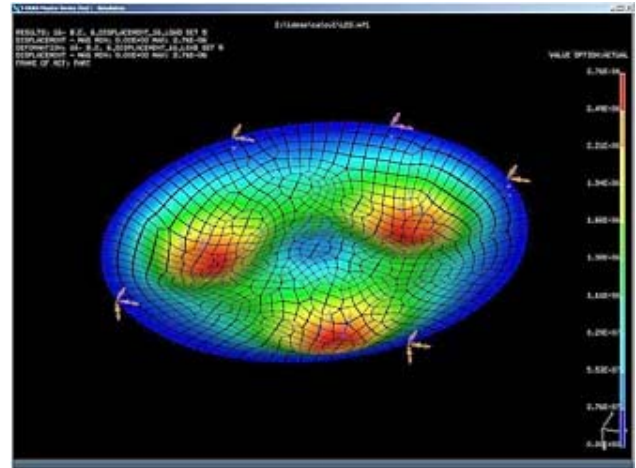


Fig. 8: Mechanical deformations modelling

The linear mechanical deformation of a deformable mirror will follow versus the excitation current with one actuator (magnet / winding) actuated at the centre of the mirror (Fig. 9):

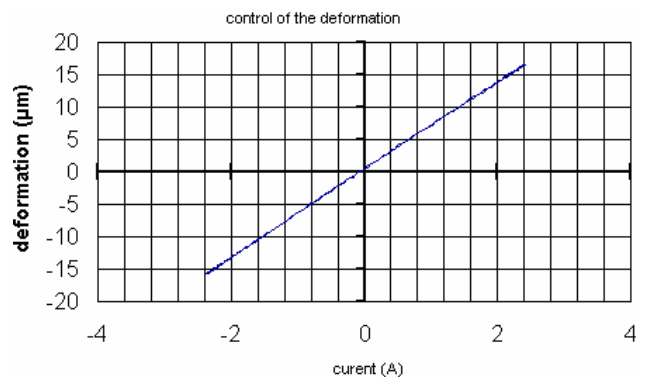


Fig. 9: Linear mechanical deformation of a deformable mirror versus the excitation current with one actuator (magnet / winding) actuated at the centre of the mirror

The frequency response of the deformable mirror will follow (Fig. 10):

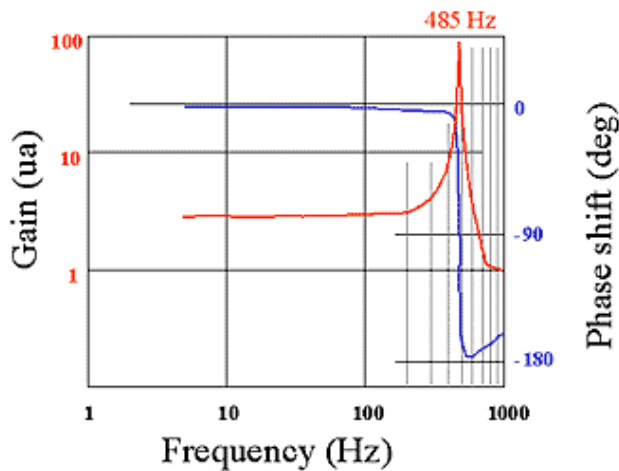


Fig. 10: Frequency response of the deformable mirror

## 8. Perspectives: Integration of MEMS in design and robust optimal control schemes (the case of design and robust optimal control of smart beams with application on vibrations suppression)

### 8. 1. Introduction

A self-adaptive structure, which reacts to the environment and minimises the effect of the applied disturbances is characterised as smart or intelligent structure. Vibration control of structures is essential to achieve optimal design with desirable performance. Passive damping treatments have been used extensively in many structural systems to reduce vibration response. Once the damping treatments are installed, the damping cannot be adjusted. Recently, active damping control has received increasing attention of its ability to provide adjustable and significant damping that traditional passive damping treatments cannot. By taking into account the continuing price reduction of electronic components and devices, one recognises the considerable saving, which can be achieved in comparison with classical, passive design. In the development of smart structural systems, piezoelectric materials are widely used as sensors and actuators for the purpose of self-controlling the structural response. A detailed review on the shape control of structures, with focus on smart structures with piezoelectric control actuation is given in Refs. [20,21]. One attractive way for vibration suppression of flexible structures is the bonding or incorporation

into the structure of a large number of active, lightweight, distributed sensors and actuators made of piezoelectric material. Piezoelectric actuators are considered to be suitable for cases which require the quick application of relatively low control forces, as an example in the reduction of wind effects or noise suppression. The investigations in this field have focussed mainly on the analyses of beams and plates with bonded sensors and actuators which operate according to a chosen control law [22–26]. The choice of the control technique is important in designing controllers which ensure the suitable functioning of the flexible structures under required conditions and at the same time can be easily applied. One main class of controllers considered in the vibration control literature are linear feedback controllers. Moreover, uncertainty in the parameters of the mechanical system or in the loading is an acceptable fact of life. In addition, one would like to follow the dynamical response by as few measurements (sensors) as possible. These facts should be taken into account during the design of the control strategy. Therefore, robust control methods are more suitable than classical ones.

The study of the vibration control in a beam is important since the beam is a fundamental structural element. In this work, a laminated beam with piezoelectric sensors and actuators is modelled by the finite element method and the performance of the active vibration control is studied. The problem of active control is studied using classical optimal control using LQR to obtain optimal control gains [26–27]. This paper also is concerned with the problem of designing a robust  $H_2$  linear feedback controller for vibration control in a flexible beam.  $H_2$  optimal control technique uses as performance measure the  $H_2$  norm, defined in the frequency domain for a stable transfer matrix. Since the worst case cost is minimized by this approach it is very natural performance criterion in considered vibration control problem. Further models have been discussed, among others, in Refs. [21, 26, 28]. The effect of the piezoelectric material properties on active control performance is studied.

### 8. 2. Numerical results

In order to test the accuracy of the presented model and control approaches a slender cantilever beam discretized with four finite elements under ambient vibration and sinusoidal wind-type loading is considered. The beam has the following actuator/sensor configuration: a pair of piezoelectric patches is bonded symmetrically at the top and the

bottom surfaces of each beam element. The top and the bottom piezoelectric layers are positioned with identical poling directions for effective sensing and strong actuation.

The effectiveness of these types of active beam elements in suppressing the vibration of the laminated beam is investigated below for Euler-Bernoulli model using LQR and H2 control strategies. For demonstration purposes the smart beam is assumed to be of rectangular cross section with length 0.8 m, width 0.02 m and height 0.005 m. Material constants for the host beam are: Elastic modulus (GPa) 73, density (kg/m<sup>3</sup>) 2700. A viscous damping coefficient equal to 0.01 is considered. Both the top and bottom layers have the same thickness of 0.002 m. Moreover the piezo - ceramic elastic modulus (GPa) 69, the charge constant  $d_{31}$   $210 \times 10^{-12}$  m/V and a voltage constant  $11.5 \times 10^{-3}$  Vm/N are assumed. The disturbances influence the displacement and the rotational degrees of freedom.

Three kinds of dynamic loading are used as disturbances.

The first one is an impact load of 2 N distributed in the free end of the cantilevered beam for 1 ms duration. The second one simulates a strong wind and is periodic sinusoidal loading pressure acting on every node on one side of the structure. (It corresponds to the technical recommendation with  $r_0=0.125$  N/m<sup>2</sup>;  $v_m=16.0$ ;  $g=2.504$ ;  $c=Z1.0$ ;

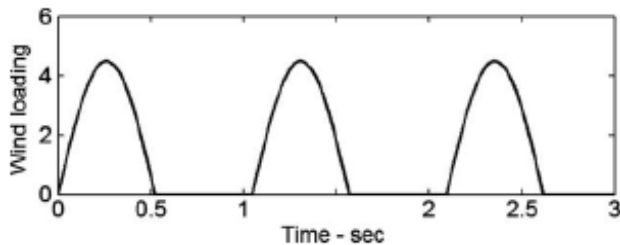


Fig. 11: Schematic representation of the dynamical system.

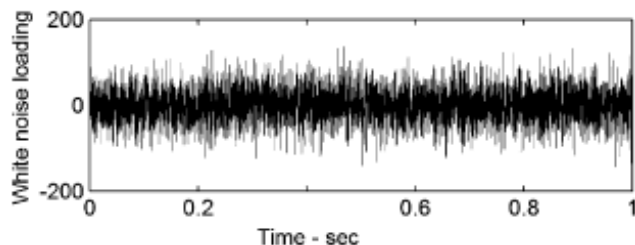


Fig. 12: Sinusoidal periodic impulsive vertical wind-type pressure.

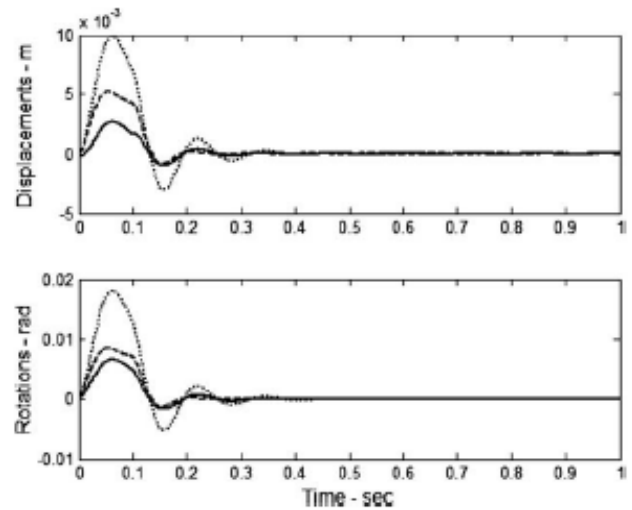


Fig. 13: Plots of the displacements and rotations for the free (dot), LQR (dash) and H2 (solid) controlled beam tip.

$p_w=0.5 \cdot r_0 \cdot v_m \cdot \Lambda^2 \cdot (1+g) \cdot c_f \cdot \sin(t)$  according to Ref. [29]). The shape of this loading is shown in Fig. 11. The third dynamic loading is random white noise with zero mean acting on each node of the beam (Fig. 12). The response of the open-loop system and the responses of the closed-loop system for the different loadings and the two proposed control strategies are compared.

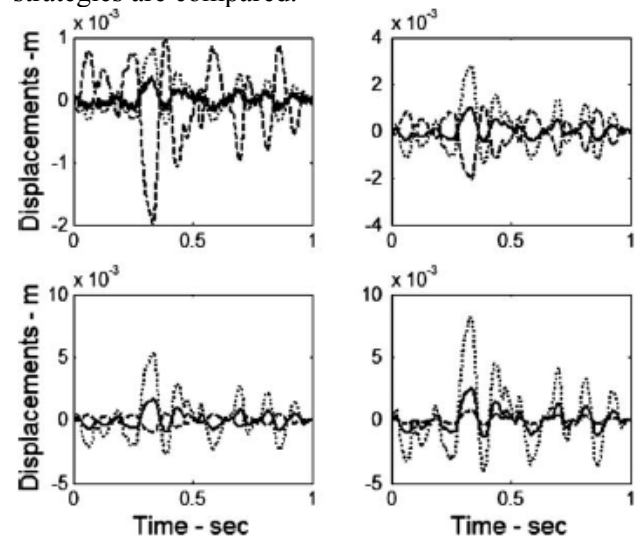


Fig. 14: Displacements for the four nodes of uncontrolled (dot) and controlled H<sub>2</sub> law with (dash) and without (solid) amplifier due to random loading.

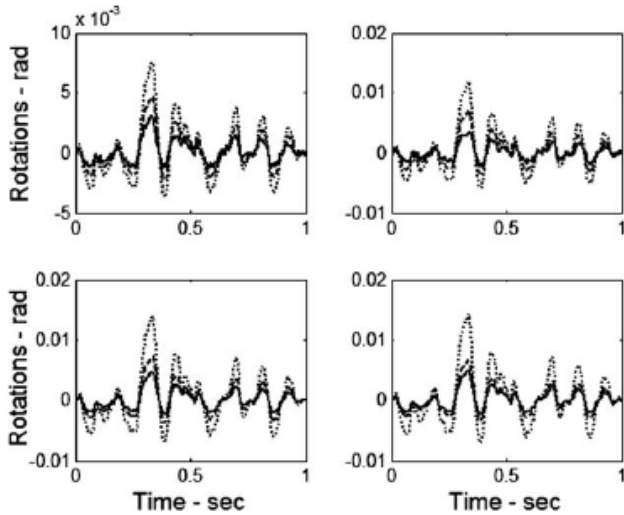


Fig. 15: Rotations for the four nodes of uncontrolled (dot) and controlled  $H_2$  law with (dash) and without (solid) amplifier due to random loading.

The comparison is based on the reduction of the magnitude of the maximum vertical displacements and rotations.

All simulation cases illustrate asymptotic stability of both control strategies. This is expected. Only available states are used for the design of the LQR control gain as well as for the organization of the control and filter gains in the  $H_2$  case. This leads to heavy penalization of the control in the LQR performance criterion ( $R=r \cdot I_{4 \times 4}$ ,  $r=0.000001$ ), i.e. enhanced vibration suppression ability of the controller.

Applying an impulsive constant load we observe that the two control laws very quickly suppress the vibrations bringing the system very close to the equilibrium. Better results are obtained with  $H_2$  control law. The LQR law reduces the vertical displacements by 38.04% versus 79.35% for  $H_2$  control law. Rotations are reduced by 44.72% using LQR and by 56.52% using  $H_2$  control law. The results for the beam tip are displaced in Fig. 13.

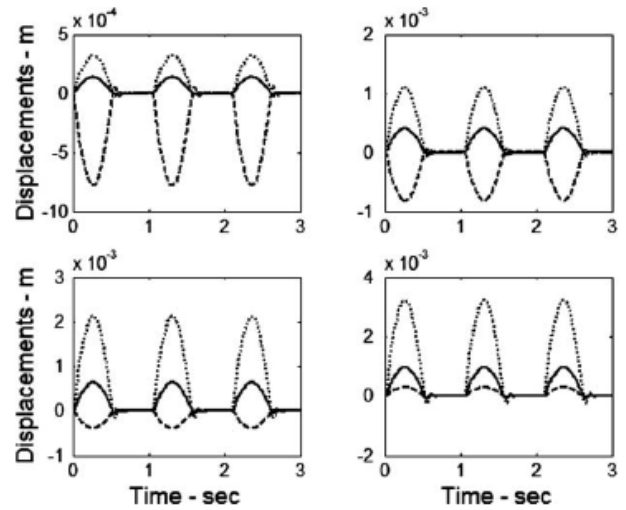


Fig. 16: Displacements for the four nodes of uncontrolled (dot) and controlled  $H_2$  law with (dash) and without (solid) amplifier due to sinusoidal-like wind loading.

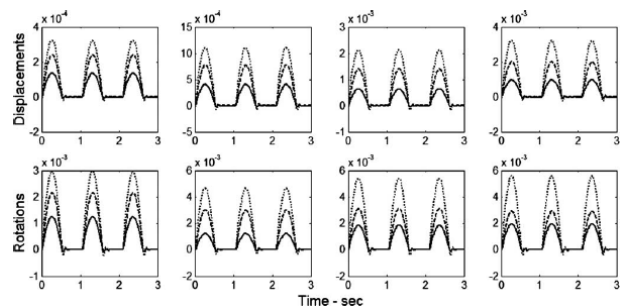


Fig. 17: Responses of the free (dot) vibrating beam and controlled beam with LQR (dash) and  $H_2$  (solid) control due to impulsive-like wind loading.

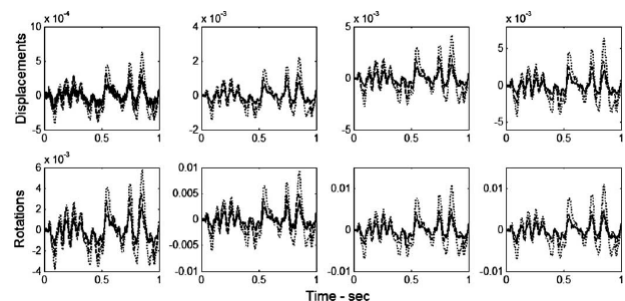


Fig. 18: The vertical displacements and rotations for all nodes for uncontrolled (dot), LQR (dash) and  $H_2$  (solid) regulated beam due to white noise loading.

When  $H_2$  controller is applied the vibrations near the free end can be efficiently suppressed. Worse results

for the vertical displacement appearing near the fixed end (dash line in the plots in Fig. 16) are due to the fact that  $H_2$  robust controller includes an estimation of the structural system from incomplete measurements and insufficient accuracy of the simplified finite element model in higher vibrational modes. This deficiency can be avoided by amplifying the first control channel and by accepting a reduced effectiveness of the vibration suppression at the free end of the beam (no more than 27%). A comparison of the displacements and rotations of the nodes for the uncontrolled beam and  $H_2$  controlled beam with and without amplification of the controller is displaced in Figs. 14 and 15 for random loading and in Figs. 16 and 17 for sinusoidal loading. Further results are considered under the assumptions that the  $H_2$  law is used with amplification of the first control channel.

Consider the behaviour of the beam subjected to sinusoidal like wind loading and regulated by both LQR and  $H_2$  control laws. The responses for the vertical displacements and for the rotations of the beam are shown in Fig. 17. The maximum vertical displacement in the controlled structure is reduced by 37.5% using LQR approach and by 71.43% using  $H_2$  law. For the reduction of the maximum rotation these values are 48.21 and 74.48%, respectively.

Results for all nodes of the uncontrolled and controlled by the two-control strategies beam subjected to white noise are given in Fig. 18. The maximum vertical displacement in the controlled structure is reduced by 50.68% using LQR and 67.12% and  $H_2$  law. The maximum rotation deflection is reduced by 58.73% and by 66.67%, respectively.

A detailed investigation of the dynamical response of active beams and other structures will give us confidence in order to propose concrete industrial applications. Among others, suppression of wind vibrations and noise reduction in lightweight (e.g. aluminium) facades in architecture and civil engineering can be achieved by means of the proposed method. More advanced results towards the same direction may be found in Ref. [30].

## 9. Conclusion

In this paper, an electrical - thermal MEMS microactuator modelling is presented. The ambition of the author was to explain, how ANSYS Multiphysics capabilities fits into the Microsystem/MEMS design process. Basic characteristics of the behaviour of such a microactuator were identified. A further step of study will be to take into account the dependence of

the electric conductivity on temperature. This paper presents the mathematical formulation and the computational model for the active vibration control of a slender beam bonded with piezoelectric sensors and actuators too. It is given as a perspective to the MEMS technology towards the direction of integrating MEMS in design and robust optimal control schemes. A finite element model has been developed for the beam structure. LQR optimal control has been applied to study the vibration control performance. In order to achieve robustness with respect to external disturbances and uncertainties of the system or of the loading, an  $H_2$  optimal control problem is investigated. Proper selection of the involved parameters is very important for a successful design of this controller. The comparison between the two proposed control laws shows that both strategies are effective. The second method is preferred due to the aforementioned robustness properties. The numerical simulations show that the proposed methods are usable for vibration suppression of a laminated beam subjected to wind-induced loading.

### References:

- [1] M.-H. Bao and W. Wang, Future of microelectromechanical systems (MEMS), *Sens Actuators, A* **56** (1996), pp. 135–141.
- [2] Liu C. Micro electromechanical systems (MEMS): technology and future applications in circuits. In: Proceedings of the IEEE fifth international conference on solid-state and integrated circuit technology, 1998. p. 928–31.
- [3] Sugiyama S. Synchrotron radiation micro lithography and etching (SMILE) for MEMS fabrication. In: Proceedings of the IEEE international conference on microprocesses and nanotechnology, 2001. p. 264–5.
- [4] Arjun Selvakumar, Khalil Najafi and Vertical comb array microactuators, *J Micro-electromech Syst* **12** (2003) (4), pp. 440–449.
- [5] H. Debeda, T.V. Freyhold, J. Mohr, U. Wallrabe and J. Wengelin, Development of miniaturized piezoelectric actuators for optical applications realized using LIGA technology, *IEEE J Microelectromech Syst* **8** (1999) (3), pp. 258–263.
- [6] E. Quandt and K. Seemann, Fabrication and simulation of magnetostrictive thin-film actuators, *Sens Actuators, A* **50** (1995), pp. 105–109.
- [7] J.W. Judy and R.S. Muller, Magnetic microactuation of torsional polysilicon structures, *Sen Actuators, A* **53** (1996), pp. 392–397.
- [8] W. Riethmüller and W. Benecke, Thermally excited silicon microactuators, *IEEE Trans Electron Dev* **35** (1988) (6), pp. 758–763.

- [9] Fujita Hiroyuki. Studies of micro actuators in Japan. In: Proceedings of the IEEE international conference robotics and automation, Scottsdale, AZ USA, 1989. p. 1559–64.
- [10] E. Thielicke and E. Obermeier, Microactuators and their technologies, *Mechatronics* **10** (2000), pp. 431–455.
- [11] Poddar AK, Pandey KN. Microwave switch using MEMS-technology. In: Proceedings of the IEEE eighth international symposium on high performance electron devices for microwave and optoelectronic application, 2000. p. 134–9.
- [12] Goldsmith C, Ehmke J, Pillans B, et al., Lifetime characterization of capacitive RF MEMS switch. In: IEEE MTT-S international microwave symposium digest, Phoenix, AZ, 2001, p. 227–30.
- [13] C. Liu, Development of surface micromachined magnetic actuators using electroplated permalloy, *Mechatronics* **8** (1998), pp. 613–633.
- [14] T.S. Chin, Permanent magnet films for applications in microelectromechanical systems, *J Magn Magn Mater* **209** (2000), pp. 75–79.
- [15] W.P. Taylor, O. Brand and M.G. Allen, Fully integrated magnetically actuated micromachined relays, *IEEE J Microelectromech Syst* **7** (1998) (2), pp. 181–191.
- [16] Williams J, Wang W. UV-LIGA fabrication of electromagnetic power micro-relays. In: Proceedings of the international symposium on test and measurement, 2001. p. 1–9.
- [17] M. Ruan, J. Shen and C.B. Wheeler, Latching microelectromagnetic relays, *Sens Actuators, A* **91** (2001), pp. 346–350.
- [18] H. Ren and E. Gerhard, Design and fabrication of a current-pulse-excited bistable magnetic microactuator, *Sens Actuators, A* **58** (1997), pp. 259–264.
- [19] C. Divoux, PhD Thesis, presented at the Laboratoire d'Electrotechnique de Grenoble, Ecole Nationale Supérieure d'Ingenieurs Electriciens de Grenoble, Institut National Polytechnique de Grenoble, 1998 (IN FRENCH).
- [20] Irschik H. A review on static and dynamic shape control of structures by piezoelectric actuation. *Eng Struct* 2002; 24:5–11.
- [21] Rao SS, Sunar M. Recent advances in sensing and control of flexible structures via piezoelectric material technology. *Appl Mech Rev* 1999;52:1–16.
- [22] Aldraihem OJ, Wetherhold RC, Singh T. Distributed control of laminated beams: Timoshenko theory vs. Euler-Bernoulli theory. *J Intell Mater Syst Struct* 1997; 8:149–57.
- [23] Foutsitzi G, Marinova D, Hadjigeorgiou E, Stavroulakis GE. Finite element modeling of optimally controlled smart beams 28th summer school: applications of mathematics in engineering and economics, Sozopol, Bulgaria, June 8–11, 2002 Bulvest 2000 press and faculty of applied mathematics and informatics. Sofia: Technical University of Sofia; 2003. p. 199–207.
- [24] Lee CK. Theory of laminated piezoelectric plates for the design of the distributed sensors/actuators. Part I. Governing equations and reciprocal relationships. *J Acoust Soc Am* 1990; 87:1144–58.
- [25] Preumont A. Vibration control of active structures. Dordrecht: Kluwer Academic Publishers; 1997.
- [26] Arvanitis KG, Zacharenakis EC, Soldatos AG, Stavroulakis GE. In: Belyaev A, Guran A, editors. New trends in optimal structural control. Selected Topics in Structronic and Mechatronic System. Singapore: World Scientific Publishers; 2003. p. 321–416 [chapter 8].
- [27] Lin C-C, Haung H-N. Vibration control of beam-plates with bonded piezoelectric sensors and actuators. *Comput Struct* 1999;73: 239–48.
- [28] Foutsitzi G, Marinova D, Hadjigeorgiou H, Stavroulakis GE. Robust H-2 vibration control of beams with piezoelectric sensors and actuators. Physics and control conference, St. Petersburg, Russia, 20–22.08.2003. vol. 1, 2004. p. 157–62.
- [29] Baniotopoulos CC, Plalis TA. Wind actions on civil engineering structures according to eurocode 1-2.4 and applications on slender structures.: KTIRIO-Scientific Publication A; 2002. p. 61–8.
- [30] Hadjigeorgiou EP, Stavroulakis GE, Massalas CV. Shape control and damage identification of beams using piezoelectric actuation and genetic optimization. : *International Journal of Engineering Science* 44 (2006) 409–421.